Analysis of Ultrasound Backscatter from Ensembles of Cells and Isolated Nuclei

Michael C. Kolios[1,2], Gregory J. Czarnota[1], Mohammed Hussain[2], F. Stuart Foster[2], John W. Hunt[2] and Michael D. Sherar[2], [1]MPCS Dept. Ryerson University, Toronto, Canada M5B 2K3 and [2]Medical Biophysics, University of Toronto, Toronto, Canada M5G 2M9

Abstract-- We have previously shown that the intensity of the ultrasound backscatter from cells ensembles undergoing apoptosis increases and shifts in their normalized power spectra are detected when compared to the backscatter from non-apoptotic cells. The etiology of these changes is unknown. During apoptosis many cellular changes occur, perhaps the most striking being the condensation and subsequent fragmentation of the cell nucleus. In this set of experiments have exposed either whole Acute Myeloid Leukemia (AML) cells or nuclei isolated from AML cells to different ionic strengths known to induce specific and reproducible cellular and nuclear changes. Ultrasound images and rf backscatter data were collected and analyzed at the different ionic strengths, and electron micrographs were made. Exposing cells to higher ionic strengths increased the ultrasound backscatter by 12 dB, but exposing the nuclei to the same experimental conditions decreased the backscatter by 23 dB. Furthermore, while the spectral slopes of the rf backscatter were similar for cells and nuclei at physiological saline, at increased concentrations the slope increased for the nuclei but decreased for the cells. The paper discusses the implications and significance of the findings. In conclusion, disruptions in cell and nuclear structure induced by exposure to strong ionic environments can greatly alter the ultrasound backscatter signal characteristics.

I. INTRODUCTION

Conventional ultrasound imaging is based on envelope detection of echoes generated from ultrasonic scatterers in tissues. Ultrasonic backscatter is generated by spatial variations in tissue density and sound propagation velocity - the tissue acoustic impedance. Echo components from aggregates of unresolved scatterers give rise to the complex speckle pattern detected during ultrasound imaging. Analysis of the spectral content of these echoes should give some information regarding the physical characteristics of the scatterers (such as size, shape and acoustical properties) and their distribution in space.

We have shown[1, 2] that ultrasonic backscatter increases in cell ensembles undergoing apoptosis after chemotherapeutic exposure (when compared to cells not exposed to the drug), and their there is a shift in power of their power spectra towards higher frequencies[3, 4]. We hypothesize that changes in the nucleus of the cell are mainly responsible for the detected differences. The nuclear condensation and fragmentation that occurs during apoptosis has two consequences: a) a change in the physical properties of the scatterers and b) a change in the randomization of the condensed nuclear material within the nucleus.

In the experiments presented the ionic environment of cells and isolated nuclei were modified. The changes in the ionic environments produced specific changes in cell and nuclear structure, and we investigated how these changes altered the backscatter signals detected.

II. METHODS

A. Biological Specimens

Cells were prepared using a cell culture system. Approximately $1x10^9$ human acute myeloid leukemia cells (AML-5) were grown in α-minimal-media from frozen stock samples for the cell experiments. Cell culture growth was initiated using frozen stock cells. The cells were then pelleted and prepared for imaging by immersing the pellet in a PBS solution of the appropriate salinity. Here we present the results from cells and isolated nuclei (details on the procedure of nuclear isolation can be found elsewhere[5]) exposed to normal salinity (0.9% w/v NaCl) and increased salinity (7.2% w/v NaCl). After the ultrasound imaging and spectroscopy experiments the cells were fixed for Haematoxylin and Eosin and electron microscopy staining.

B. Ultrasound data collection

The imaging was performed using a custom-built high frequency ultrasound imager[6]. A 5 mm diameter 35 MHz f/2 transducer was used in these experiments with a -15dB bandwidth of approximately 100% (23 - 48 MHz) and a radius of curvature of approximately 9 mm.

0-7803-7177-1/01/$10.00 © 2001 IEEE

In these experiments 12-bit 500 MHz rf data were acquired along at least 35 independent locations in the cell/nuclei pellets using an oscilloscope (Lecroy 9362 Model). Each stored a-scan was the temporal average of 100-200 echoes to decrease noise. Matlab (Natick, MA, USA www.mathworks.com) was used to perform signal analysis. The region of interest (ROI) was centered approximately at the transducer focus and was approximately 1 mm in length. The Fourier transform of the ROI was taken using a Hamming window. The power spectrum was obtained by averaging the results from the independent scan lines. This power spectrum was divided by the power spectrum of the echo from a calibration target (quartz flat). Linear regression analysis was applied, in a manner similar to that proposed by Lizzi *et.al.*[7]. The spectral slope (the slope of the linear regression of the calibrated spectrogram) and the mid-band fit (the value for the spectral amplitude at the transducer operating frequency) were calculated. Assuming a random distribution of weak scatterers (Born approximation), these parameters can be related to the physical characteristics of the ultrasound scatterers. An increase in the spectral slope corresponds to a decrease in *effective* scatterer size while the mid-band fit is a function of the scatterer shape, size, acoustic impedance and concentration. Further details on the technique, as well as theoretical and signal analysis considerations can be found elsewhere[7-10].

III. RESLUTS

A superposition of the rf data recorded by our system (at least 30 independent scan lines) are shown in Figure 1. At normal salinity, the backscatter signal intensity (as measured by the mid-band fit) from the isolated nuclei pellets was ~20 dB greater than that from the cell pellets (Table 1). Upon exposure of the cells to 7.2% w/v NaCl, the backscatter signal from the cell pellets increased by 12dB while the signal from the nuclei decreased by 23 dB (Figure 1 and Table 1). Furthermore, while the spectral slope values for the cell and isolated nucleus pellets were similar at normal salt concentrations (Table 1), at 8 times the salinity the spectral slope from the cell pellet backscatter decreased by a factor of 2 while the spectral slope of the rf data from the isolated nucleus pellet increased by a factor of 2.

The experimental values of the mid-band fit and spectral slope can be compared to theoretical values if the physical characteristics of the transducer and the ultrasound scatterers are known[3]. A comparison of the values obtained in Table 1 with theoretical results is currently under investigation and we are conducting experiments to characterize ultrasonically AML cells

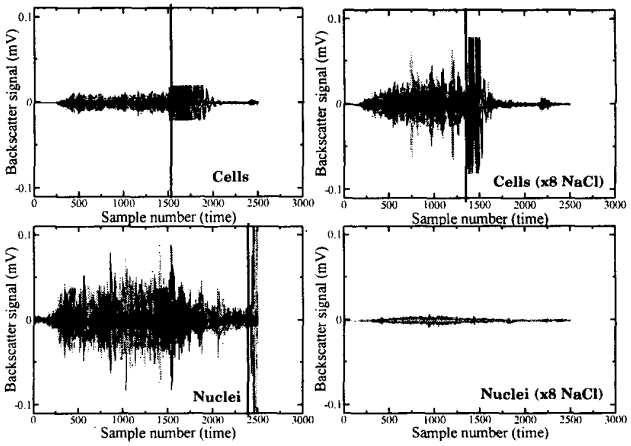

Figure 1: Plot of rf data (at least 30 scans superimposed) collected from four pellet samples: cells and nuclei at normal saline concentrations (two left panels) and at x8 saline concentrations (two right panels). Solid black vertical lines correspond to locations that an ultrasound reflector was located for characterization measurements (not discussed here).

and their isolated nuclei. Assuming that the scatterers are small and weak (Born approximation), isotropic (in this case spherical) and randomly positioned in space, the standard deviation of the measurements can be calculated. This calculation is shown in the last row of Table 1 and is in reasonable agreement with the experimental values.

Transmission Electron Microscopy (TEM) of individual cells and nuclei from the experiments is shown in Figure 2. For cells at normal saline the nuclear membrane is intact, the central nucleolus can be seen, and there is no apparent chromatin condensation within the nucleus; this is typical interphase staining. After exposure of the cells to the increased salinity, there is a collapse of the cytoplasm (cell shrinking), partial disruption of the nuclear membrane, and condensed chromatin distributed throughout the nucleus (Figure 2B). The impact of the high ionic environment is more dramatic for the isolated nuclei. Individual nucleui exposed to 7.2% w/v NaCl (Figure 2C, different magnification) show the unraveling of the chromatin structure and weak nuclear staining. The nuclear membrane is disrupted, but still intact.

	Mid-Band fit	Spectral Slope
Cells	-45 +/- 1.7 dB	0.42 +/- 0.17dB/MHz
Cells x8	-33 +/- 1.6 dB	0.19 +/- 0.19 dB/MHz
Nuclei	-25 +/- 2.3 dB	0.41 +/- 0.19 dB/MHz
Nuclei x8	-48 +/- 1.7 dB	0.87 +/- 0.13 dB/MHz
Theor. SD	*1.2 dB*	*0.18 dB/MHz*

Table 1: Mid-band fit and spectral slope (+/- 1 SD) for pellets of cells at physiological and increased (x8) saline concentrations and for nuclei pellets at physiological and increased (x8) saline concentrations. Theoretical values[7] for the expected standard deviation of the measurements in shown in the last row.

IV. Discussion

Striking changes were measured in the intensity and spectral characteristics of the backscatter rf signals from pellets of cells and isolated nuclei exposed to increased salt concentrations. These ionic changes result in disruptions in the structure of the cell and nuclear material and specific changes in nuclear structure[5]. Some of these changes can be seen in figure 2.

What can explain the differences in the rf signals detected? The ultrasound wavelength for the 34 MHz transducer used (assuming a speed of sound of 1.5 mm/μs) is 44 μm. The sizes of the scatterers are unknown, since it is not even known what structures predominantly scatter the ultrasound at the frequencies. Since the cell diameters are 6-10 μm, one can assume that the scatterers are smaller than this. We have however accumulated strong evidence that structural transformations within the cell nucleus are responsible for these changes. If one assumes a random distribution of scatterers in each case examined, then an increase in backscatter is the result of an increase in the size, concentration and acoustic impedance of the ultrasonic scatterers. If the scatterers are not random[11, 12], then the problem becomes more complex, and not amendable to the theoretical analysis we have used.

Assuming that the nucleus is the major scatterer, the differential of 20 dB in backscatter from cells to nuclei at normal salinity is likely due to an increase in scatterer concentration. There is no strong reason to assume a change in scatterer size or acoustic impedance. Furthermore, the fact that in both cases the spectral slope is the same would indicate similar *effective* scatterer radii. From these numbers, estimates about the number of scatterers can be made.

When the whole cells are exposed to the higher salt concentrations, they shrink in size approaching the size of the individual nuclei and there is increased nuclear condensation. Furthermore, the backscatter increases by 12 dB and the spectral slope decreases by half. This would indicate that the changes are due to larger effective scatterers with increased cross sections (due to the slope and the condensed regions seen in the TEM). When nuclei are exposed to the same ionic concentration, the backscatter drops by 23 dB to levels slightly lower than those of cells in normal saline. Interestingly, the slope in this case doubles, indicating very small Rayleigh scatterers are contributing to the signal.

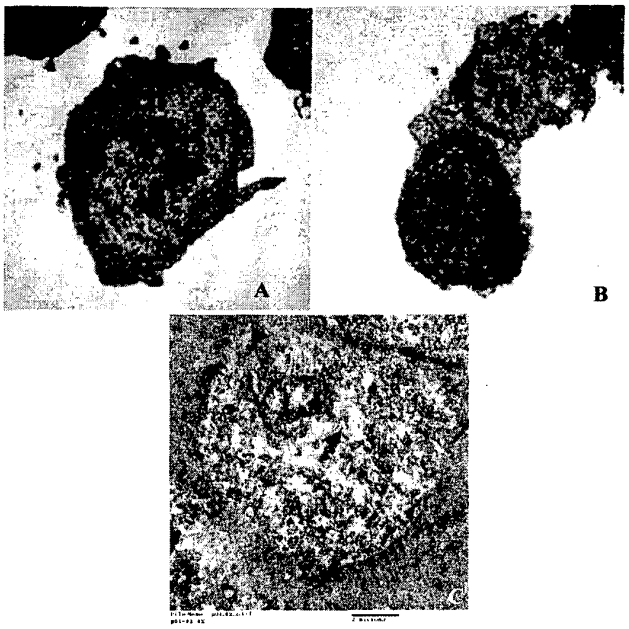

Figure 2: Transmission Electron Micrographs of a cell at normal saline (panel A) and increased (x8) saline (panel B). The electron microscopy of an isolated nucleus at increased saline concentration is presented in panel C (bar 2 μm).

If the scatterer distribution is not random, the above conclusions do not hold. In this case, the changes in the backscatter intensity will also be related to the degree of randomization of the ultrasonic scatterers[12-14]. This makes the analysis more complex since not only do the scatterers have to be identified, but also their degree of randomization determined. We are currently preparing experiments by which individual cells are trapped in a gel at a concentration sufficiently low so that on average only one cell would be in the ultrasound resolution cell, thereby avoiding randomization effects. By trapping normal, apoptotic cells or isolated nuclei previously exposed to various agents in such a gel, changes in the rf signals could be attributed to changes in the scatterer

size and composition only, and not their distribution in space.

Better knowledge of why the changes in rf signal characteristics occur will enable us to optimize the technology and use ultrasound imaging and spectroscopy systems with the appropriate frequencies, excitation pulses and signal analysis and classification algorithms to detect whether apoptosis or other cellular events that involve changes in nuclear structure occur. Applications of this technology include cancer treatment monitoring, organ transplant assessment and monitoring apoptosis in developmental models.

V. CONCLUSIONS

We have demonstrated that the structural changes that cells and isolated nuclei undergo when exposed to different salt concentrations can change the backscatter intensity by 10-30dB and double or half the spectral slope values when compared to the values at physiological salt concentrations. The data provide further evidence to the importance of nuclear structure on ultrasound backscatter at these high frequencies.

ACKNOWLEDGMENTS

The authors would like to acknowledge the financial support of the Canadian Institute for Health Research, the National Sciences and Engineering Research Council of Canada.

REFERENCES

[1] Czarnota, G.J., et al., *Ultrasonic biomicroscopy of viable, dead and apoptotic cells.* Ultrasound Med Biol, 1997. **23**(6): p. 961-5.

[2] Czarnota, G.J., et al., *High-frequency ultrasound imaging of apoptosis in vitro, in situ, and in vivo.* Faseb Journal, 1999. **13**(7): p. A1436-A1436.

[3] Kolios, M.C., et al., *Ultrasound spectral parameter imaging of apoptosis.* Ultrasound in Medicine & Biology, 2001(Submitted).

[4] Kolios, M.C., et al., *Ultrasonic spectrum analysis of apoptotic cell populations.* Faseb Journal, 1999. **13**(7): p. A1435-A1435.

[5] Czarnota, G.J. and F.P. Ottensmeyer, *Structural states of the nucleosome.* J Biol Chem, 1996. **271**(7): p. 3677-83.

[6] Sherar, M.D., M.B. Noss, and F.S. Foster, *Ultrasound backscatter microscopy images the internal structure of living tumour spheroids.* Nature, 1987. **330**(6147): p. 493-5.

[7] Lizzi, F.L., et al., *Statistical framework for ultrasonic spectral parameter imaging.* Ultrasound Med Biol, 1997. **23**(9): p. 1371-82.

[8] Feleppa, E.J., et al., *Diagnostic spectrum analysis in ophthalmology: a physical perspective.* Ultrasound Med Biol, 1986. **12**(8): p. 623-31.

[9] Lizzi, F.L., et al., *Theoretical framework for spectrum analysis in ultrasonic tissue characterization.* J Acoust Soc Am, 1983. **73**(4): p. 1366-73.

[10] Lizzi, F.L., et al., *Comparison of theoretical scattering results and ultrasonic data from clinical liver examinations.* Ultrasound Med Biol, 1988. **14**(5): p. 377-85.

[11] Hunt, J.W., et al., *A model based upon pseudo-regular spacing of cells combined with the randomization of nuclei can explain the significant changes in high-freqeuncy ultrasound signals during apoptosis.* Ultrasound in Medicine & Biology, 2001(Submitted).

[12] Hunt, J.W., A.E. Worthington, and A.T. Kerr, *The subtleties of ultrasound images of an ensemble of cells: simulation from regular and more random distributions of scatterers.* Ultrasound Med Biol, 1995. **21**(3): p. 329-41.

[13] Mo, L.Y., et al., *Ultrasound scattering from blood with hematocrits up to 100%.* IEEE Trans Biomed Eng, 1994. **41**(1): p. 91-5.

[14] Narayanan, V.M., et al., *Studies on ultrasonic scattering from quasi-periodic structures.* IEEE Transactions on Ultrasonics, Ferroelectrics and Frequency Control, 1997. **44**(1): p. 114-24.